# Electron detachment of negative ions: The influence of the outermost electron and its neutral core atom in collision with He, Ne, and Ar

Ginette Jalbert, W. Wolff, S. D. Magalhães, and N. V. de Castro Faria
*Instituto de Física, Universidade Federal do Rio de Janeiro, Caixa Postal 68528, Rio de Janeiro, 21941-972 RJ, Brazil*
(Received 4 October 2007; published 29 January 2008)

A systematic investigation of the absolute total detachment cross sections of atomic negative ions is presented and a simple semiclassical model developed based on the experimental findings. The total electron detachment process for several anion species, namely $C^-$, $O^-$, $F^-$, $S^-$, $Si^-$, $Cl^-$, $Ge^-$, and $Na^-$, in collisions with He, Ne, and Ar, in the velocity range of 0.2–1.8 a.u., were studied. In the intermediate-velocity regime the experimental data are well reproduced by the proposed model, which assumes independent contributions from the outermost quasifree electron and from the neutral core atom of the negative ion.

DOI: 10.1103/PhysRevA.77.012722 PACS number(s): 34.50.Fa, 34.90.+q

## I. INTRODUCTION

Most collision measurements of atomic negative ions with rare-gas atoms study the production of neutral atoms or of positive ions. Single and double electron detachment cross sections have been measured for several negative ions colliding with gas targets, mainly in the velocity range below 0.5 a.u., by several authors. Almost all initial studies dealing with negative ions have been focused on $H^-$ and $He^-$ colliding with atoms or molecules [1–3]. Electron-loss cross sections for $C^-$ and $O^-$ have been measured using the beam attenuation technique for anions in the energy range of 1–30 keV [4,5]. For heavier atomic negative ions, particularly in the intermediate-velocity range, most of the total detachment cross sections available in the literature have been reported by us [6–8]; the only previously reported total detachment measurements are the ones from Andersen [9], for negative alkali-metal ions.

In the low-velocity region, where a molecular or quasimolecular description is valid, a reasonable understanding has been achieved [10], and in the zero and short-range potential approximations [11–15] calculations were able to fit well the measured cross sections for $H^-$ and $F^-$ colliding with atomic and molecular targets [16]. At the other extreme, in the high-velocity region, the impulse approximation and the free collision model [17–19] have been applied with some success for light negative ions. Since no quantitative theory exists, in the intermediate-velocity range for heavier negative ions, qualitative interpretations were attempted and scaling models proposed [6,7,9,20], but only now a clearer picture of the detachment process in this velocity range is beginning to emerge.

In the last few years we have systematically measured absolute total electron detachment cross sections of atomic negative ions, of the second and third period of the periodic table of elements, colliding with noble gases [6–8] in the intermediate-velocity range of 0.2–1.8 a.u. In our last work we pursued the problem by measuring and analyzing the detachment process of atomic and cluster anions of Al, Si, and C, colliding only with Ar [21]. This work has shed light on the problem.

The main process, namely direct detachment of the valence electron leaving behind a neutral atom, has given us some clues as how to approach the problem. First, in the detachment process from negative ions, with or without a clearly defined single last shell electron, one of the outermost electrons plays a significant role. Second, the other important part is related to the electronic cloud of the neutral core of the anion.

The present study complements the before mentioned work. We extended our study to several atomic anions colliding with He and Ne targets, including Ar again. The aim of this paper is to discuss the observed similarities between electron-impact and negative-ion collisions on rare-gas targets, and to present a semiclassical model for the absolute total electron detachment (TED) cross sections, based on the experimental findings.

All detachment cross sections, measured in the LaCAM laboratory with the usual beam attenuation technique, have already been published elsewhere [6–8]. The experimental technique, developed by our group, has been previously described in detail [22].

## II. SEMICLASSICAL MODEL

### A. Experimental findings

For He, Ne, and Ar targets available total detachment cross sections of $Li^-$, $B^-$, $C^-$, $O^-$, $F^-$, $Al^-$, $S^-$, $Si^-$, $Cl^-$, and $Ge^-$ negative ions are separately displayed in Fig. 1 for each target, as a function of the anion velocity $v_p$, in atomic units. Only for the sake of comparison, the experimental data were scaled by multiplicative factors $X^i_{\text{target}}$ to the fluorine anion data, which present the smallest cross sections. This scaling procedure provided us the required link to the electron impact cross sections, as has been already pointed out elsewhere [21]. As can be seen in the figure, the experimental data points cluster within a band, suggesting a general trend.

In the case of the He target, Fig. 1(a), the normalized TED cross sections show an overall decrease as a function of the velocity, while for the Ne target, Fig. 1(b), the opposite behavior is observed. Rather broad maxima occur, around 0.5 and 1.7 a.u., for He and Ne, respectively. A more peak-shaped structure is present in the Ar case, located approximately at 1.1 a.u., as displayed in Fig. 1(c). However, it should be pointed out that the applied scaling procedure

 

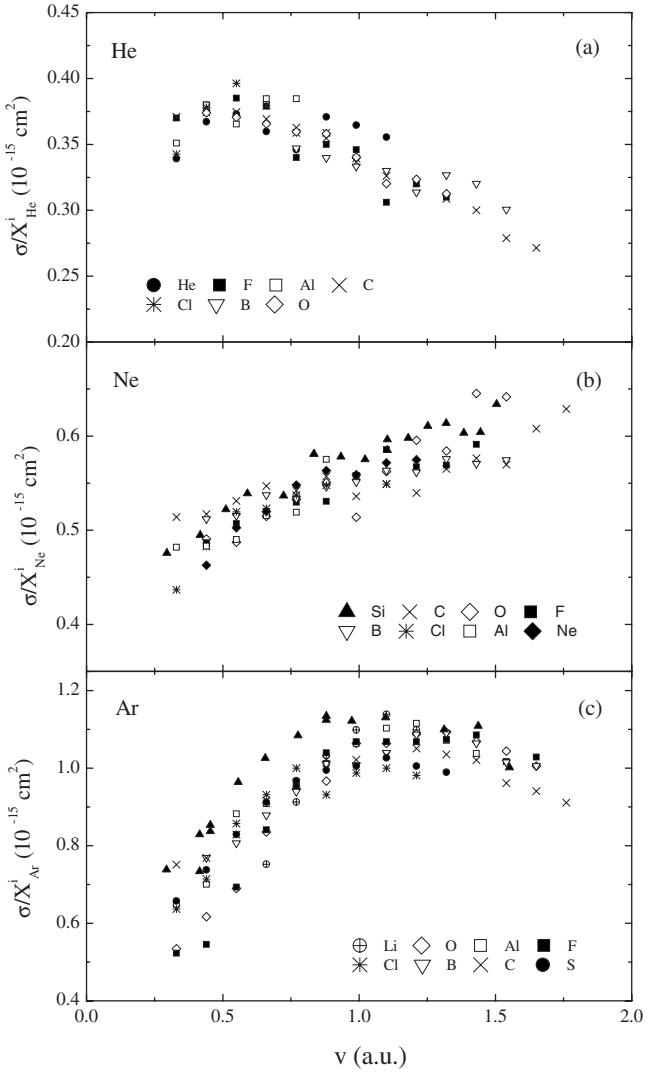


FIG. 1. Total electron detachment cross sections for the several $np^m$ anions, normalized to the fluorine values, incident on He (a), Ne (b), and Ar (c), as a function of the relative velocity in atomic units.

somehow distorts the shape of the cross section curves; they are less or more widened, depending on the scaling factor.

By comparing the experimental data with the corresponding electron impact cross sections for He, Ne, and Ar [23–26], it becomes clear that the TED cross sections follow the trend of the electron impact cross sections. This is surprising, considering the wide selection of anions with different electronic configurations ($np^3$, $np^5$, $np^6$, $ns^2$), and electron affinities varying between 0.28 and 3.6 eV [27]. A question at this point is to what extent each negative ion species, with its particular electronic configuration and electron affinity, is reflected in the detachment cross section. The basic difference between electron impact and negative ion collision experiments lies in the electron velocity distribution; in the former case monoenergetic electrons are incident on the targets, while in the latter the anion's electrons possess a wide velocity distribution.

As in all experiments the final state of the target has not been measured, the electron impact cross sections include both elastic and inelastic contributions. Actually, in the velocity range studied in the present work, the main contribution to the electron impact cross sections is due to elastic scattering [26,28–30]. In the following section, we will proceed with the description of a semiclassical model.

### B. Basis of the model: Role of the outermost electron and the core effect

The negative ion is modeled as a single outermost electron, plus a neutral core mimicked by an impenetrable sphere. From a classical point of view, the outermost electron of the anion is attached to the core as a quasifree electron, orbiting around it with a velocity distribution related to its electronic state. It is also implicit in this picture that no correlations are considered between the least bound electrons, and between them and the core electrons.

In order to obtain the outermost electron velocity distribution, quantum mechanical concepts have been introduced. The spatial wave functions of the least bound electrons $\psi(\vec{r})$ have been taken from wave function tables of Clementi and Roetti [31]. They are given by a linear combination of Slater type orbitals $\chi_i(\vec{r})$:

$$\psi(\vec{r}) = \sum_{i=1}^{i=N} C_i \chi_i(\vec{r}) \tag{1}$$

with

$$\chi(\vec{r}) = N(\zeta,k) r^{k-1} e^{-\zeta r} Y_{l,m}(\theta_r, \phi_r), \tag{2}$$

where $N(\zeta,k)=[(2k)!]^{-1/2}(2\zeta)^{k+1/2}$, with $\zeta$ and $N$ chosen for the electronic orbital with the lowest energy and $Y_{l,m}(\theta,\phi)$ are the spherical harmonics. The basis functions are factorized into a radial $R(r)$ and an angular part:

$$\psi(\vec{r}) = \sum_{i=1}^{i=N} C_i f_i(r) Y_{l_i,m_i}(\theta_r, \phi_r). \tag{3}$$

The Fourier transform of $\psi(\vec{r})$ is then obtained as a linear combination of the Fourier transform of the Slater orbitals:

$$\Psi(\vec{k}) = \sum_{i=1}^{i=N} C_i \phi_i(\vec{k}), \tag{4}$$

where

$$\phi(\vec{k}) = \frac{1}{(2\pi)^{3/2}} \int e^{i\vec{k}\cdot\vec{r}} f(r) Y_{l,m}(\theta,\phi) d\vec{r}. \tag{5}$$

According to Bransden and Joachain [32] the function $\phi(\vec{k})$ is deduced from

$$\phi(\vec{k}) = (i)^l \frac{4\pi}{(2\pi)^{3/2}} F(k) Y_{lm}(\theta_k, \phi_k) \tag{6}$$

with

$$F(k) = \int_0^\infty f(r) j_l(kr) r^2 dr \tag{7}$$

and $j_l(kr)$ being the Bessel spherical functions. Finally, the wave function in momentum space becomes

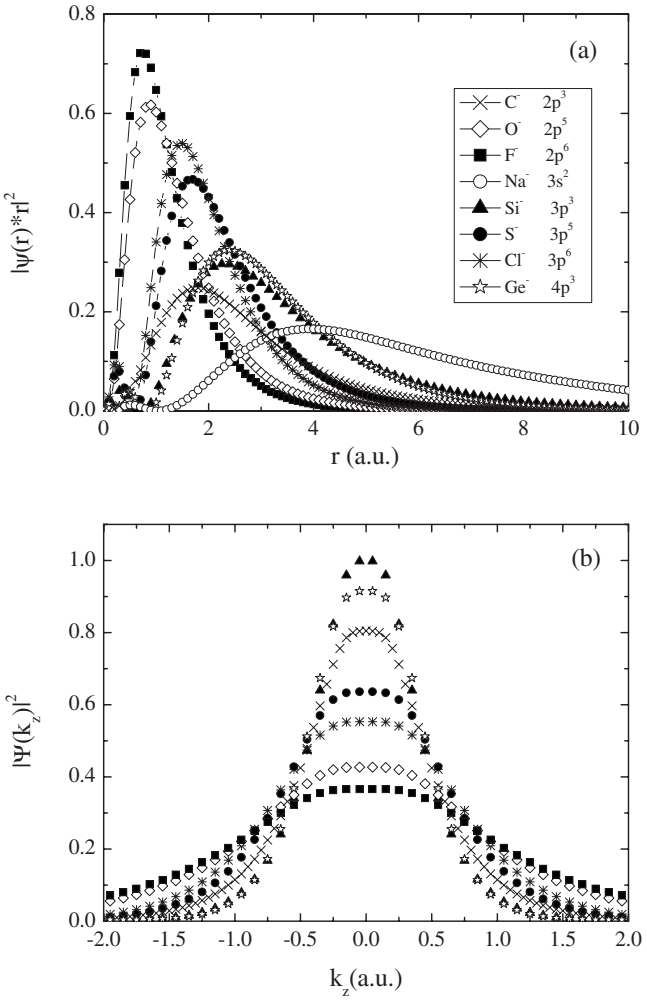


FIG. 2. (a) Radial distribution functions for $C^-$, $O^-$, $F^-$, $Na^-$, $Si^-$, $S^-$, $Cl^-$, and $Ge^-$. (b) Squared modulus of the Fourier transform of the outermost electron's wave function, integrated over the perpendicular directions to the beam direction, for the same anions.

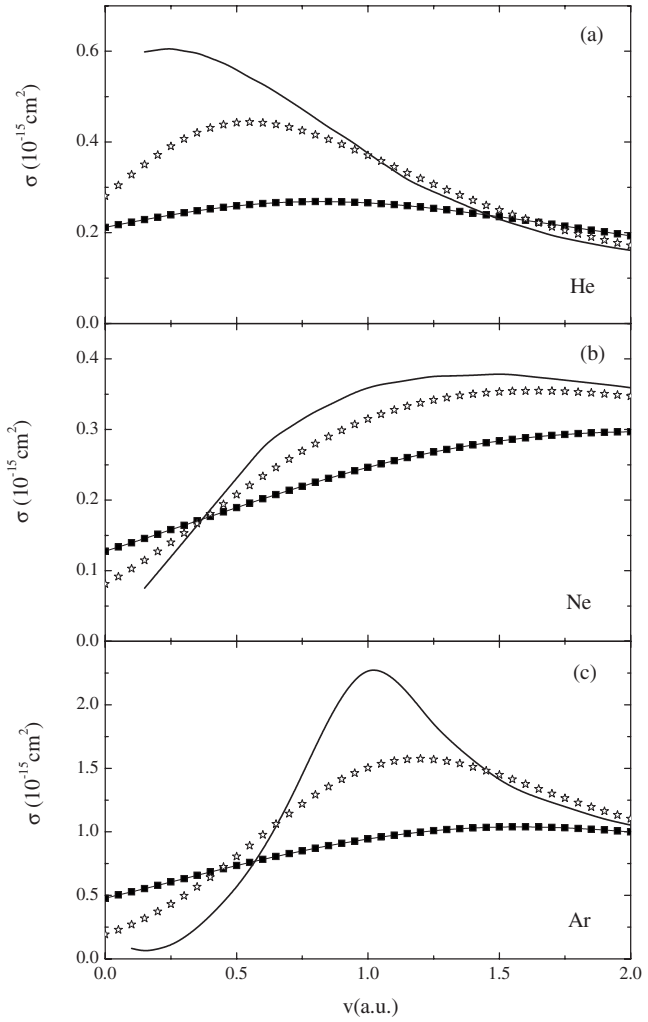


FIG. 3. Total scattering cross sections of free electrons (full line), Refs. [23–26]; convolution with outermost electron's velocity distribution: $Ge^-$ (open star) and $F^-$ (full square). Targets: He (a), Ne (b), and Ar (c).

$$\Psi(\vec{k}) = \sum_{i=1}^{i=N} C_i F_i(k) Y_{l_i m_i}(\theta_k, \phi_k). \tag{8}$$

It is worth mentioning that $F_i(k)$ can be analytically calculated.

In Fig. 2(a) the radial distribution functions $|\psi(r)|^2 r^2$ of the least bound electron of $C^-$, $O^-$, $F^-$, $S^-$, $Si^-$, $Cl^-$, $Ge^-$, and $Na^-$ are displayed. The squared modulus of the Fourier transform of the electronic wave function $|\Psi(k_z)|^2$, integrated over the perpendicular directions to the beam direction ($z$), as a function of the momentum in the beam direction ($k_z$), is shown in Fig. 2(b) for each negative ion. Although they are of similar shape, their widths depend strongly on the anion electronic orbital, as expected from the radial distributions.

In order to obtain what we call here the outermost electron detachment (OED) cross section, it is necessary to perform a convolution of the electron impact cross section of each target (He, Ne, and Ar) with the velocity distribution of the outermost electron in the anion rest frame, $g(v-V)$:

$$\sigma_{\mathrm{OED}}^{\mathrm{model}}(v) = \int \sigma_{\mathrm{electron}}(V) g(v-V) dV, \tag{9}$$

where

$$g(v-V) = |\Psi(v-V)|^2 \tag{10}$$

with $V=k_z$, expressed in atomic units.

The electron impact cross sections of He, Ne, and Ar [23–26] are displayed in Figs. 3(a)–3(c), respectively, together with the calculations of the OED cross sections of fluorine and germanium anions. Those anions possess, respectively, the widest and narrowest velocity distribution widths, as shown in Fig. 2(b). The broadening effect of the convolution is clearly discernible.

The next step is then to compare the experimental TED cross sections with the calculated OED cross sections, for all collision systems, and to verify the consistency of the proposed model. To make the problem simple to handle, it is assumed in the model that the total electron detachment cross

section $\sigma_{\mathrm{TED}}(v)$ is separable into two major cross sections, one contribution coming exclusively from the outermost electron $\sigma_{\mathrm{OED}}(v)$ and the other one $\sigma_{\mathrm{NCD}}(v)$ coming from the neutral core of the negative ion:

$$\sigma_{\mathrm{TED}}^{\mathrm{model}}(v) = \sigma_{\mathrm{OED}}^{\mathrm{model}}(v) + \sigma_{\mathrm{NCD}}(v). \tag{11}$$

It must be emphasized that the outermost electron detachment cross section (OEDCS) is not directly related to the single electron detachment cross section (SEDCS). The single electron detachment (SED) process is not restricted only to the loss of the outermost electron, but includes the loss of any other electron. The weakly bound electron is more likely to be detached in the process, but its contribution to the SEDCS has not yet been measured.

The neutral core detachment (NCD) cross section contains the contribution from multiple electron detachment plus SED of a nonoutermost electron. As has been already pointed out, the neutral core of the negative ion was considered as a sphere. In addition we assume, in a first approximation, the electronic cloud to be close-packed. Therefore to estimate the neutral core detachment cross section (NCDCS), it is sufficient to define a pure geometrical cross section

$$\sigma_{\mathrm{NCD}}^{\mathrm{geo}} = \pi(R_{\mathrm{gas}} + R_{\mathrm{neutral}})^2, \tag{12}$$

and a modified geometrical cross section

$$\sigma_{\mathrm{NCD}}^{\mathrm{model}} = \alpha\sigma_{\mathrm{NCD}}^{\mathrm{geo}}, \tag{13}$$

where $R_{\mathrm{gas}}$ and $R_{\mathrm{neutral}}$ are the radii of the gas target atom and of the neutral anion, both adopted from [33], and $\alpha$ is a parameter to be extracted from the experimental data. The NCD contribution to the TEDCS is assumed to be proportional to a purely geometrical cross section. In that case, the parameter $\alpha$ is simply a measure of the overlap between the electronic clouds of the neutral core and of the target atom. By assuming that the NCDCS is constant for given collision partners implies that it has no influence on the shape of the TEDCS dependence on the collision velocity. Along these lines a crude estimate of atom-atom collision cross sections is being proposed, for the intermediate-velocity regime.

In the case of atom-atom collisions, ionization processes occur when the electronic clouds of the atoms overlap. The ionization proceeds through two competing mechanisms: scattering of the electrons by the partially screened cores or scattering between target and projectile electrons. At low velocities, the former dominates [34,35].

It should be noted that what we call here the outermost electron detachment process is not necessarily the dominating electron detachment mechanism; either the OED or the NCD process can be more likely.

## III. RESULTS AND DISCUSSION

In the case of Ar, excellent agreement has been found among all experimental results and the model calculations,

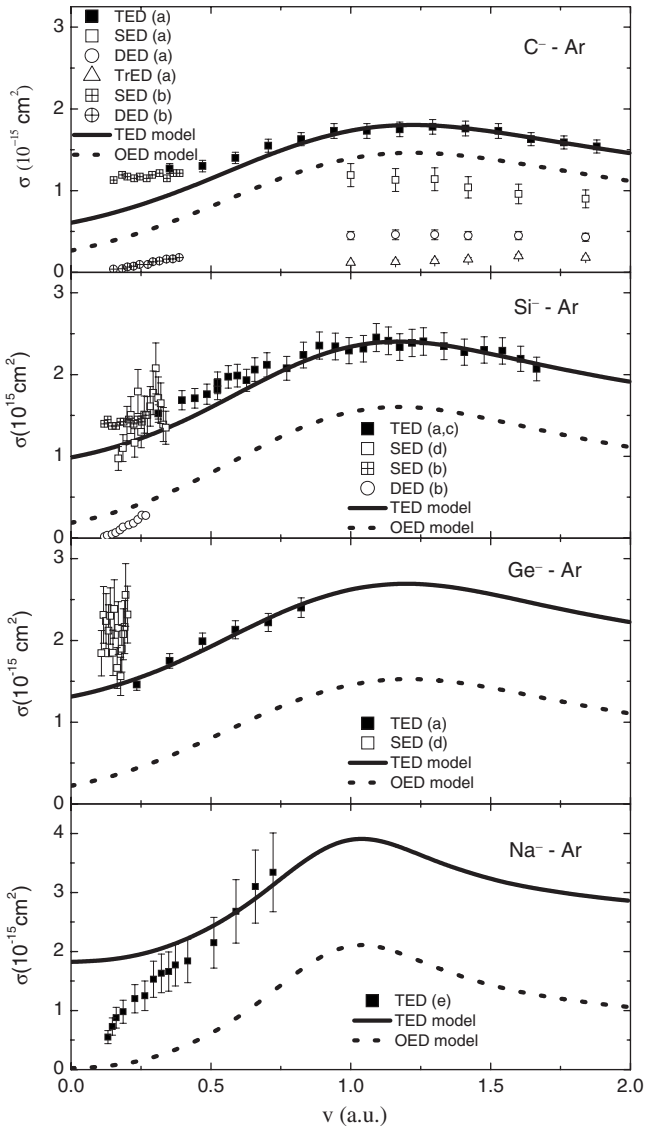


FIG. 4. Argon target experimental and model cross sections. References: (a) Ref. [8], (b) Ref. [41], (c) Ref. [7], (d) Ref. [40], (e) Ref. [9]. TED model [Eq. (11)] and OED model [Eq. (9)], from present work.

within the experimental error limits, as shown in Figs. 4 and 5, giving strong support to the proposed approach to describe the TEDCS. The broad peak feature, evident in all experimental cross section curves, is in complete agreement with the model predictions for its shape and maximum position. That maximum is centered approximately at $v_p$=1.15 and 1.3 a.u., for the anions in the $np^3$ and $np^5$-$np^6$ subshell configuration, respectively. For the anion in the $ns^2$ configuration the cross section maximum is expected to be around 1.0 a.u., but unfortunately the available experimental data do not reach this velocity range. In the measured low-velocity range region a systematic deviation is present, establishing a lower limit (at around $v_p$=0.4 a.u.) for the validity of the model.

In Fig. 4, all collision data involving negative ions in $np^5$ and $np^6$ configurations [6,36–39] and in Fig. 5, those belonging to $np^3$ and $ns^2$ configurations [7–9,40,41], are displayed. The figures show the experimental total electron detachment

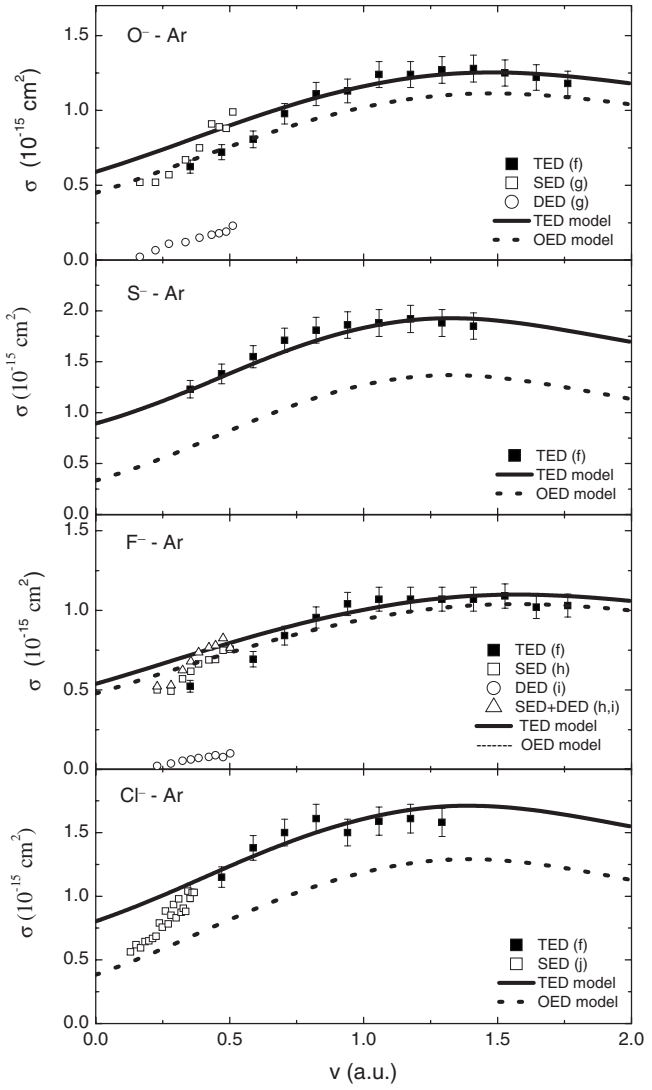


FIG. 5. Argon target experimental and model cross sections. References: (f) Ref. [6], (g) Ref. [36], (h) Ref. [37], (i) Ref. [38], (j) Ref. [39]. TED model and OED model, from present work.

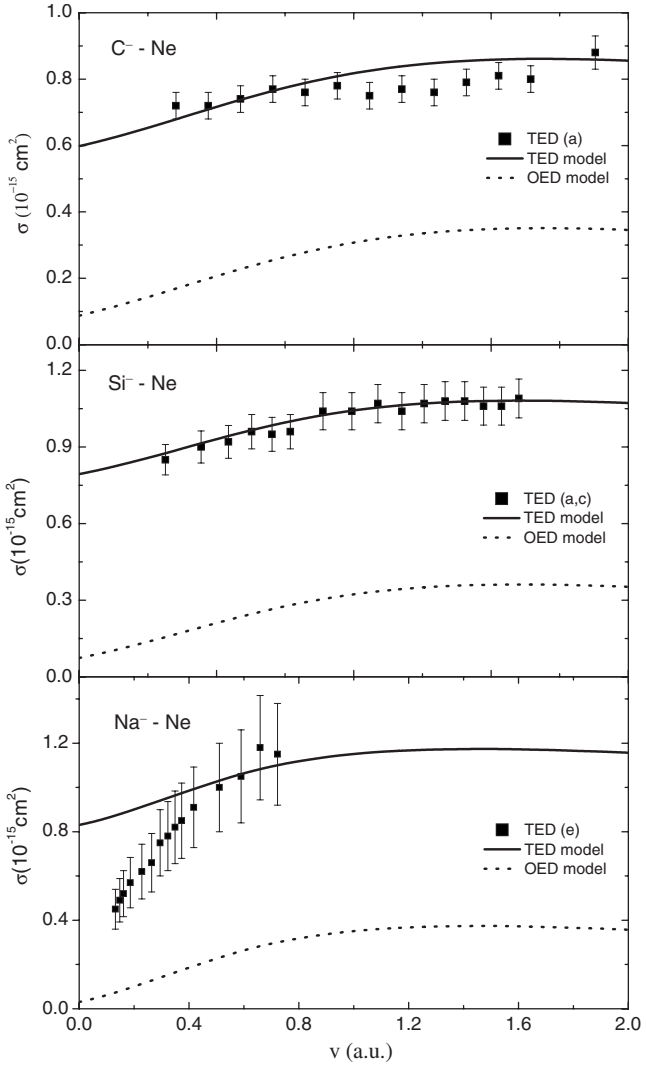


FIG. 6. Neon target experimental and model cross sections. References: (a) Ref. [8], (c) Ref. [7], (e) Ref. [9]. TED model and OED model, from present work.

cross sections, as well as the single and double detachment cross sections, together with the model calculations for the outermost electron and total electron detachment cross sections. The calculated OEDCS describes well the shape of the experimental TEDCS, but not its absolute value. A constant term must be added to the calculated OEDCS that corresponds directly to the NCDCS. It follows from both figures that the velocity independent NCDCS increases with the size of the anion's neutral core atom.

Those general features remain unchanged for all the seven negative ion species with nonzero angular momentum ($l$) and, unexpectedly, the same is true for the anion with $l=0$. A discrepancy between model and experiment would be expected, considering that the $np^3$ electrons and even more the $3s^2$ electrons should present some correlations, but this expectation is not confirmed. Therefore all outer shell electrons seem to behave independently, indicating an apparent lack of any strong correlation between them in the intermediate-velocity regime, starting at $v_p=0.4$ a.u.

In order to illustrate the relative importance and velocity dependence of the different detachment channels, SED and multiple electron detachment cross sections for the $C^-$ anion are included in Fig. 4(a) [8]. The double and triple detachment cross sections remain essentially constant along the measured velocity range.

For the Ne case, starting also at $v_p=0.4$ a.u., there is close agreement between the calculations and the experimental data sets of total detachment cross sections [6–9] within the experimental errors, as shown in Figs. 6 and 7. The calculated and experimental TEDCS increase with the velocity toward a slight indication of a maximum around $v_p=1.7$ a.u., for the anions with a $np^5$-$np^6$ subshell configuration; and around a lower value $v_p=1.5$ a.u. for the anions with a $np^3$ configuration. A better experimental determination of it could not be accomplished due to the upper limit of velocity available to us [6–8]. Above $v_p=1.0$ a.u., both experimental and calculated cross sections are very flat for the Ne target case. Experimental SED and double electron detachment (DED) cross sections were also included [36–39].

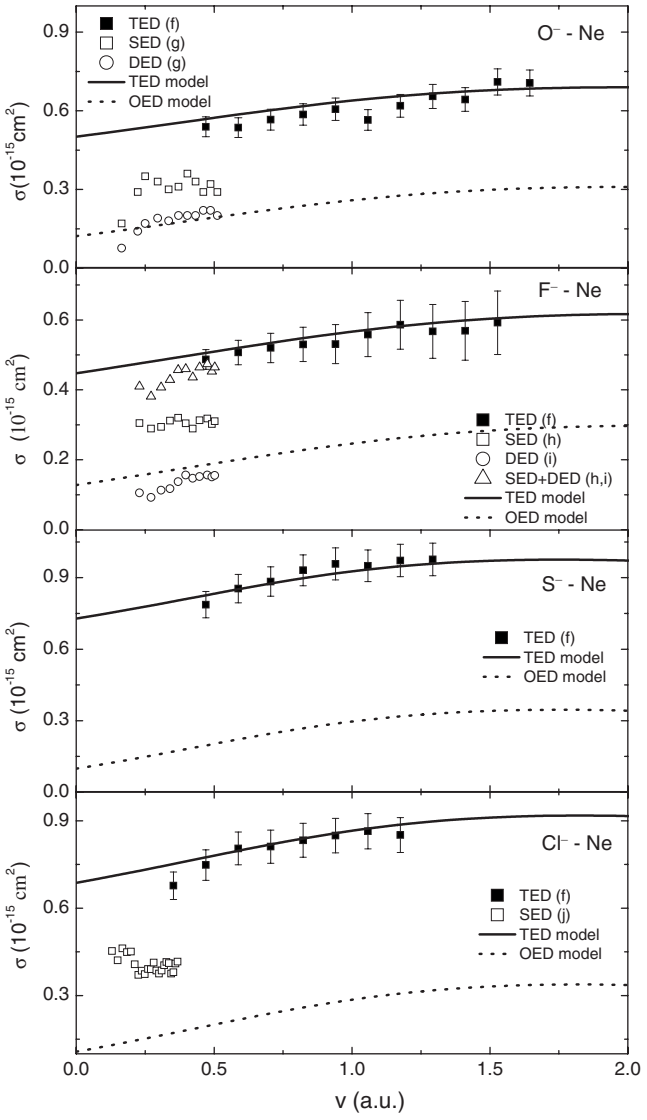


FIG. 7. Neon target experimental and model cross sections. References: (f) Ref. [6], (g) Ref. [36], (h) Ref. [37], (i) Ref. [38], (j) Ref. [39]. TED model and OED model, from present work.

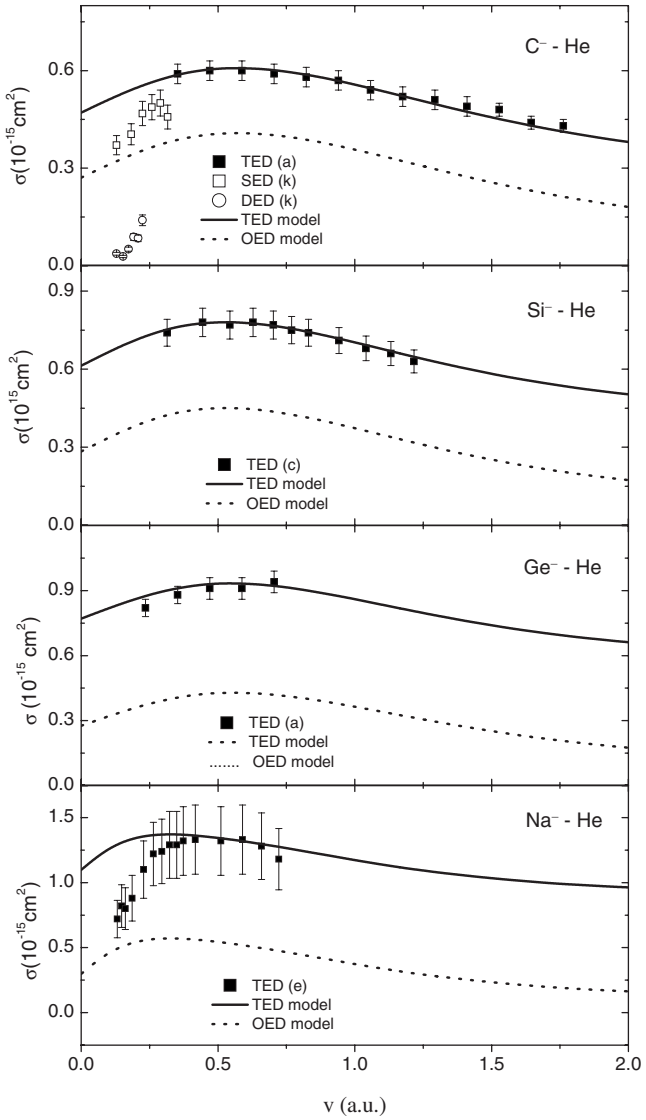


FIG. 8. Helium target experimental and model cross sections. References: (a) Ref. [8], (c) Ref. [7], (e) Ref. [9], (k) Ref. [43]. TED model and OED model, from present work.

For the He case, the total detachment cross sections also agree well with the model calculations, within the experimental uncertainties, as shown in Figs. 8 and 9. In contrast to the Ne case, both experimental and calculated cross sections show a gradual decrease with the velocity. The maxima are expected to be located in the low-velocity range, within the interval $v_p=0.45-0.6$ a.u., for the $p$-orbital anions. The SED and DED experimental results were added [36–39,42,43].

For the selected negative ions, measurements of SEDCS and DEDCS available in the literature, most of them measured in the low-velocity range (from 0.1 to 0.4 a.u.), have been included in the figures for comparison. If added together, the sum does not always join smoothly to the low-velocity TED experimental results [6–8]. Those discrepancies can be partly accounted for by difficulties in normalizing data from different measurements, or by the different experimental methods employed.

Neutral-core detachment cross sections (NCDCS), as defined by Eq. (11), have been extracted from experimental TEDCS. They were then compared with the purely geometrical NCDCS, defined by Eq. (12), as depicted in Figs. 10(a)–10(c), for He, Ne, and Ar, respectively. A linear correlation between them is clearly visible, thus supporting the validity of the assumptions previously discussed in Sec. II, though the Na-Ne case exhibits a deviant value. $\alpha$ values of 0.6, 0.8, and 0.95 have then been successfully extracted for He, Ne, and Ar, respectively. As the target atomic number increases $\alpha$ tends to unity, meaning the electronic clouds get more and more closely packed. On the other hand, in the case of the He target, with $\alpha=0.6$, it is less likely that the electronic clouds behave as impenetrable spheres. For a more complete assessment of this simple picture, further measurements with Kr and Xe targets are called for.

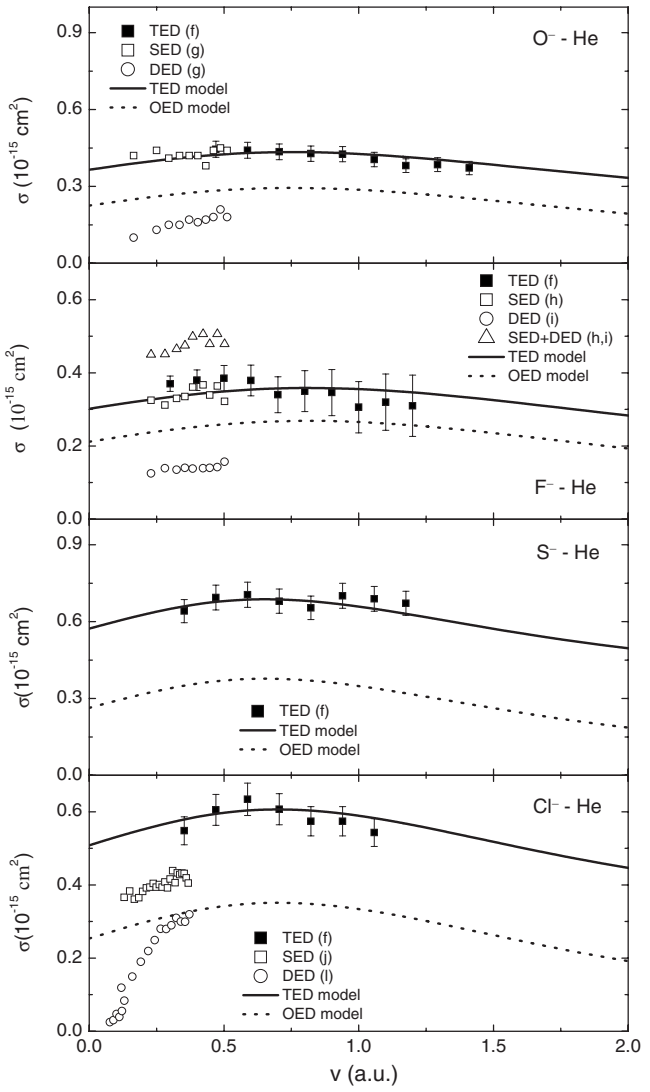


FIG. 9. Helium target experimental and model cross sections. References: (f) Ref. [6], (g) Ref. [36], (h) Ref. [37], (i) Ref. [38], (j) Ref. [39], (l) Ref. [42]. TED model and OED model, from present work.

## IV. SUMMARY AND CONCLUSIONS

The aim of this work was to obtain a comprehensive overview of the detachment process of negative ions. The shape of the total electron detachment cross section is very well reproduced by what we call here the outermost electron detachment cross section; it is thus really tempting to ascribe entirely to it the shape of the former. In order to describe all other detachment channels a geometrical cross section was tentatively proposed, with good results.

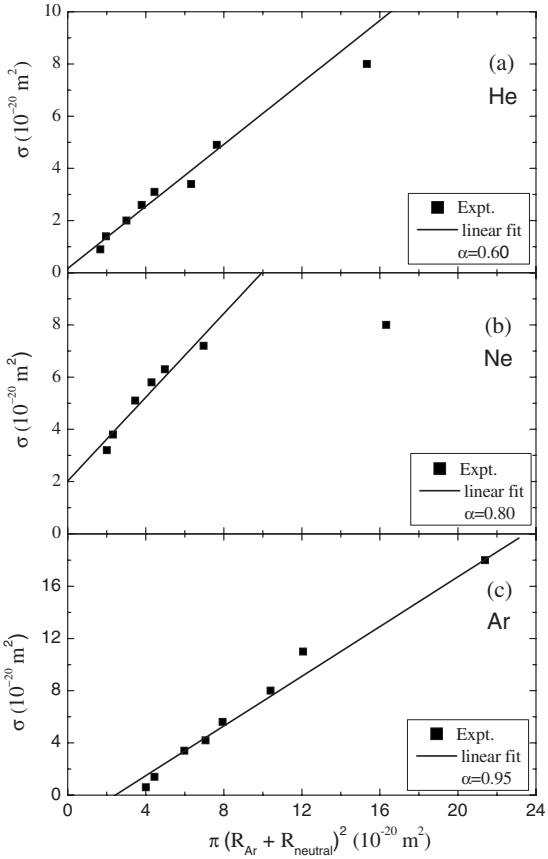


FIG. 10. Neutral-core detachment cross sections (NCDCS) vs purely geometrical cross sections, for (a) He, (b) Ne, and (c) Ar.

Though expected for some anionic species, no clear indication of correlations between the outer shell electrons has been observed, in agreement with what is expected from the model developed here. Shortcomings of the model are evident below around $v_p=0.4$ a.u., where we enter the low-velocity regime, but for all cases studied the model can be applied. Further investigations of the detachment process, as a function of the impact parameter, are called for to clarify the electron-electron correlation of the anionic outer shell electrons, not revealed in the present analysis.

## ACKNOWLEDGMENTS

This work was partially supported by the Brazilian agencies CNPq, FUJB, and FAPERJ.

[1] J. Sorensen, L. H. Andersen, and L. B. Nielsen, J. Phys. B **21**, 847 (1988).
[2] J. Heinemeier, P. Hvelplund, and F. R. Simpson, J. Phys. B **8**, 1880 (1975).
[3] J. Heinemeier, P. Hvelplund, and F. R. Simpson, J. Phys. B **9**, 2669 (1976).
[4] R. A. Bennett, J. T. Mosely, and J. R. Peterson, J. Chem. Phys. **62**, 2223 (1975).
[5] M. Matic and B. Cotic, J. Phys. B **4**, 111 (1971).
[6] F. Zappa, G. Jalbert, L. F. S. Coelho, A. B. Rocha, S. D.

Magalhães, and N. V. de Castro Faria, Phys. Rev. A **69**, 012703 (2004).
[7] H. Luna, S. D. Magalhães, J. C. Acquadro, M. H. P. Martins, W. M. S. Santos, G. Jalbert, L. F. S. Coelho, and N. V. de Castro Faria, Phys. Rev. A **63**, 022705 (2001).
[8] H. Luna, F. Zappa, M. H. P. Martins, S. D. Magalhães, G. Jalbert, L. F. S. Coelho, and N. V. de Castro Faria, Phys. Rev. A **63**, 052716 (2001).
[9] N. Andersen, T. Andersen, L. Jepsen, and J. Macek, J. Phys. B **17**, 2281 (1984).
[10] J. S. Risley, Proceedings of the 11th International Conference on the Physics of Electronic and Atomic Collisions, Kyoto, 1979, edited by N. Oda and K. Takayanagi (North-Holland, Amsterdam, 1980), pp. 619–630.
[11] Y. N. Demkov and V. N. Ostrovsky, *Zero-Range Potentials and Their Application in Atomic Physics* (Leningrad State University Press, Leningrad) (English translation: Plenum, New York, 1988).
[12] J. P. Gauyacq, J. Phys. B **13**, 4417 (1980).
[13] V. A. Esaulov, Proceedings of the US-Mexico Joint Seminar on the Atomic Physics of Negative Ions, edited by C. Cisneros and T. Morgan (Institute of Physics, Universidad Nacional Autónoma de México, México, 1981), p. 196).
[14] V. A. Esaulov, J. Phys. B **13**, 1625 (1980).
[15] J. P. Connerade and V. N. Ostrovsky, J. Phys. B **35**, L475 (2002).
[16] M. S. Huq, L. D. Doverspike, R. L. Champion, and V. A. Esaulov, J. Phys. B **15**, 951 (1982).
[17] D. R. Bates and J. C. G. Walker, Proc. Phys. Soc. **90**, 333 (1967).
[18] D. P. Dewangan and H. R. J. Walters, J. Phys. B **11**, 3983 (1978).
[19] M. Meron and B. M. Johnson, Phys. Rev. A **41**, 1365 (1990).
[20] F. Robicheaux, Phys. Rev. Lett. **82**, 707 (1999).
[21] G. Jalbert, L. Silva, W. Wolff, S. D. Magalhães, A. Medina, M. M. Sant'Anna, and N. V. de Castro Faria, Phys. Rev. A **74**, 042703 (2006).
[22] J. C. Acquadro, H. Luna, S. D. Magalhães, F. Zappa, G. Jalbert, L. F. S. Coelho, and N. V. de Castro Faria, Nucl. Instrum. Methods Phys. Res. B **171**, 373 (2000).
[23] S. J. Buckman and B. Lohmann, J. Phys. B **19**, 2547 (1986).
[24] J. C. Nickel, K. Imre, D. F. Register, and S. Trajmar, J. Phys. B **18**, 125 (1985).
[25] W. Y. Baek and B. Grosswendt, J. Phys. B **36**, 731 (2003).
[26] J. Yuan, J. Phys. B **21**, 3753 (1988).
[27] H. Hotop and W. C. Lineberger, J. Phys. Chem. Ref. Data **14**, 731 (1985).
[28] R. C. Wetzel, F. A. Baiocchi, T. R. Hayes, and R. S. Freund, Phys. Rev. A **35**, 559 (1987).
[29] Y. K. Kim, Phys. Rev. A **64**, 032713 (2001).
[30] S. Kaur, R. Srivastava, R. P. McEachram, and A. D. Stauffer, J. Phys. B **31**, 4833 (1998).
[31] E. Clementi and C. Roetti, At. Data Nucl. Data Tables **14**, 177 (1974).
[32] B. H. Bransden and C. J. Joachain, *Physics of Atoms and Molecules* (Longman, London, 1983).
[33] E. Clementi, D. L. Raimundi, and W. P. Reinhardt, J. Chem. Phys. **38**, 2686 (1963).
[34] E. C. Montenegro, W. S. Melo, W. E. Meyerhof, and A. G. de Pinho, Phys. Rev. A **48**, 4259 (1993).
[35] D. R. Bates, V. Dose, and N. A. Young, J. Phys. B **2**, 930 (1969).
[36] B. Hird, I. A. Abbas, and M. Bruyere, Phys. Rev. A **33**, 2315 (1986).
[37] B. Hird and F. Rahman, Phys. Rev. A **26**, 3108 (1982).
[38] B. Hird and F. Rahman, Phys. Rev. A **29**, 1541 (1984).
[39] B. Hird and F. Rahman, J. Phys. B **16**, 3581 (1983).
[40] G. Mei, Y. En-Bo, L. Yong, Z. Xue-Mei, and L. Fu-Quan, Chin. Phys. Lett. **23**, 3253 (2006).
[41] J. Ishikawa, Rev. Sci. Instrum. **63**, 2368 (1992).
[42] Y. En-Bo, G. Mei, H. Yong-Yi, W. Shi-Min, L. Guang-Wu, Z. Xue-Mei, and L. Fu-Quan, Chin. Phys. Lett. **23**, 2418 (2006).
[43] H. Yong-Yi, W. Shi-Min, Z. Xue-Mei, L. Guang-Wu, L. Fu-Quan, and Y. Fu-Jia, Chin. Phys. Lett. **21**, 1262 (2004).